Published in final edited form as:
Protein Eng Des Sel. 2016 October ; 29(10): 445–455. doi:10.1093/protein/gzw038.

Different tissue distribution properties for glycosylation variants of fusion proteins containing the p40 subunit of murine interleukin-12

F. Bootz[#], **D. Venetz**[#], **B. Ziffels**, and **D. Neri**[*]
Department of Chemistry and Applied Biosciences, Swiss Federal Institute of Technology (ETH Zürich), Vladimir Prelog Weg 1-5/10, CH-8093 Zürich (Switzerland)

[#] These authors contributed equally to this work.

Abstract

Antibody-based fusion proteins are gaining increasing importance for therapeutic applications, but the impact of glycosylation on *in vivo* biopharmaceutical performance is not always completely understood. In this article, we have analyzed biochemical and pharmaceutical properties of fusion proteins, consisting of the F8 antibody (specific to the EDA domain of fibronectin, a marker of tissue remodelling and of angiogenesis) and of the p40 subunit of interleukin-12, an inhibitor of inflammation. The corresponding fusion protein (F8-IL12p40), which inhibits colitis development in mice, is a glycosylated protein with suboptimal disease targeting properties *in vivo*. Since the protein was extensively glycosylated, as evidenced by PNGase F treatment and mass spectrometric analysis, we mutated four asparagine residues in various combinations. The corresponding proteins exhibited similar biochemical and antigen-binding properties, but differences in thermal stability and bioactivity. Asparagine mutations did not lead to recovery of disease targeting performance *in vivo*, as evidenced by quantitative biodistribution studies with radioiodinated protein preparations in tumor-bearing mice. By contrast, an almost complete recovery of targeting was achieved with an enzymatically deglycosylated protein preparation. These findings reinforce the concept that different glycostructures can have an impact on tissue distribution properties.

Keywords

biodistribution; glycoproteins; F8 antibody; immunocytokines

Introduction

The majority of small anticancer drugs and of therapeutic proteins does not preferentially localize at the tumor site after administration to patients. Indeed, many small organic drugs and biopharmaceuticals accumulate more efficiently in normal organs than in neoplastic lesions (Bosslet *et al.*, 1998, Krall *et al.*, 2013, van der Veldt *et al.*, 2010), thus leading to

[*)] corresponding author: tel: +41-44-6337401, fax: +41-44-6331358, neri@pharma.ethz.ch.

Conflict of interest statement
Dario Neri is a cofounder and shareholder of Philogen SpA (Siena, Italy), the company that owns the F8 antibody.

Europe PMC Funders Author Manuscripts

suboptimal therapeutic activity and, potentially, to side effects. For this reason, antibodies specific to tumor-associated antigens are increasingly being used as delivery vehicles, to facilitate a selective uptake of therapeutic agents at the tumor site (Schliemann and Neri, 2007, Scott *et al.*, 2012). Indeed, antibodies and their fragments have been used for the selective pharmacodelivery of various therapeutic payloads, including cytotoxic drugs (Casi and Neri, 2015, Chari *et al.*, 2014, Sievers and Senter, 2013), toxins (Alewine *et al.*, 2015), radionuclides (Steiner and Neri, 2011), cytokines (Kontermann, 2012, Pasche and Neri, 2012, Sondel and Gillies, 2012) and other immunological mediators.

The impact of glycosylation on the *in vivo* behaviour of antibodies and their derivatives has extensively been studied by pharmacokinetic analysis of serum samples, but less frequently by quantitative tissue distribution studies (e.g., using radiolabeled protein preparations). Glycoproteins containing low levels of terminal sialic acid have been reported to be cleared rapidly (Sinclair and Elliott, 2005). Additionally, receptors binding specific glycostructures, as for example the asialoglycoprotein receptor (recognizing galactosyl residues) and the mannose receptor (recognizing mannose, N-acetylglucosamine and fucose residues) can also increase protein clearance (Lee *et al.*, 2002, Morell *et al.*, 1971). We have recently reported that the absence of terminal sialic acid residues and the exposure of terminal galactosyl or N-acetylglucosamine residues abrogate targeting dramatically (Venetz *et al.*, 2015).

The conjugation of polysialic acid to various therapeutic proteins, including antibodies and antibody fragments, has been shown to increase the circulatory half-life of the corresponding products and lead, as a consequence, to improved tumor uptake (Constantinou *et al.*, 2008, Gregoriadis *et al.*, 2005). A site-specific fusion of a scFv fragment binding to carcinoembryonic antigen and a 11 kD polysialic acid chain demonstrated a 10-fold increase in tumor uptake after 24h compared to the unmodified protein, while only a minor decrease in tumor to blood ratio could be observed (Constantinou *et al.*, 2009).

Monoclonal antibodies specific to splice-isoforms of fibronectin are ideally suited for pharmacodelivery applications and for the study of extravasation kinetics. The EDA domain of fibronectin, recognized by the F8 antibody, is a stable protein, located in the subendothelial extracellular matrix of newly formed blood vessels in tumors and in other angiogenic pathological structures, while being virtually undetectable in all other murine organs (Rybak *et al.*, 2007, Schwager *et al.*, 2009, Villa *et al.*, 2008). A large variety of payloads (including drugs, cytokines and radionuclides) have been coupled or fused to antibodies, specific to fibronectin splice isoforms. The resulting products have been characterized in numerous quantitative biodistribution studies [e.g., see (Bootz and Neri, 2016, Pasche and Neri, 2012) and articles therein].

Interestingly, some antibody-based fusion proteins exhibit a complete abrogation of the tumor-targeting properties of the parental antibody. While this phenomenon may be associated to molecular size (Halin *et al.*, 2003, Poh *et al.*, 2015) or to the use of highly charged payloads (Melkko *et al.*, 2002, Niesner *et al.*, 2002), it has also been observed that heavily glycosylated fusion proteins (e.g., antibodies fused to the extracellular domain of murine CD86) are rapidly excreted via the liver and do not target tumors efficiently *in vivo*, while being fully immunoreactive *in vitro* (Hemmerle *et al.*, 2012). However, other

glycosylated antibody-based fusion proteins (e.g., those based on interleukin-4, interleukin-2 and some interleukin-9 glycoforms as therapeutic payloads) exhibited biodistribution profiles in tumor-bearing mice, which were similar to the ones of the parental antibody (Becker *et al.*, 1996, Hemmerle and Neri, 2014).

The disease targeting properties of F8 antibodies are typically assessed by quantitative biodistribution analysis in tumor-bearing mice, using radioiodinated protein preparations. It is convenient to use tumors rather than smaller pathological specimens (e.g., arthritic paws or inflamed intestine) because of easier quantification.

In this study, we describe the tissue distribution properties in tumor-bearing mice of nine fusion protein variants, consisting of the F8 antibody and of the p40 subunit of interleukin-12 (IL12). This protein payload contains four sites of N-linked glycosylation, which were removed either by PNGase F treatment or by site-directed mutagenesis (Asn-to-Gln substitution). The p40 subunit of IL12 has been reported to display a potent anti-inflammatory activity (Gillessen *et al.*, 1995, Kim *et al.*, 2012). Its fusion to the F8 antibody decreased disease severity in a mouse model of colitis (Bootz *et al.*, 2015). Despite this beneficial therapeutic effect, the fusion protein exhibited a suboptimal overall biodistribution profile, which prompted us to further investigate variants thereof.

We have found that all glycosylation-site mutants of the p40 subunit, failed to preferentially localize at the tumor site. By contrast, the F8-IL12p40 fusion protein recovered after PNGase F treatment and a diabody preparation of the F8 antibody (devoid of the p40 payload) selectively accumulated in the tumor, 24 hours after intravenous administration.

Results

Cloning, expression and characterization of the parental F8-IL12p40 fusion protein

The C-terminus of the p40 subunit of murine IL12 was fused to the N-terminus of the F8 antibody in diabody format, by sequentially joining the two corresponding gene segments with a linker sequence [Figure 1A,B, (Bootz, et al., 2015)]. In order to prevent partial covalent dimer formation, which had been observed previously, the cysteine at position 197 of the p40 moiety was mutated to a serine (C175S). The gene encoding the resulting fusion protein (hereafter named F8-IL12p40 C175S) was cloned into the mammalian expression vector pcDNA3.1 (+) [Figure 1B]. Transient gene expression in CHO-S cells (Muller *et al.*, 2007), followed by purification of the fusion protein on protein A, led to homogenous products with acceptable yields (> 14 mg/L). The purified F8-IL12p40 C175S protein was shown to be homogenous in SDS-PAGE analysis and size-exclusion chromatography [Figure 1C,D]. Surface plasmon resonance analysis revealed a high-binding affinity to the cognate antigen, which was similar to the one of the parental F8 antibody [(Villa, et al., 2008); Figure 1E]. A dose-dependent IL12 inhibitory activity was observed using F8-IL12p40 C175S in an *in vitro* assay based on interferon γ (IFNγ) production by IL12-stimulated splenocytes [Figure 1F]. Circular dichroism analysis of the purified protein confirmed the presence of anti-parallel beta sheets as secondary structure elements and revealed high thermal stability (T_m = 57°C) [Figure 1I]. A quantitative biodistribution study in mice bearing murine F9 tumors, using a radioiodinated preparation of F8-IL12p40

Europe PMC Funders Author Manuscripts

C175S, revealed poor tumor-to-organ ratios without a preferential tumor accumulation, 24 hours after intravenous administration [Figure 1G]. By contrast, the F8 antibody in diabody format exhibited substantially higher tumor-to-organ ratios at the same time point [Figure 1J].

Investigation of potential sources of limited bioavailability at the tumor site

To investigate whether the suboptimal tumor targeting properties of the F8-IL12p40 C175S fusion was caused by binding to erythrocytes or leukocytes, a comparative blood incubation assay was performed, using radioiodinated preparations of F8-IL12p40 C175S and of F8 in diabody format. After 1 h incubation in blood and a centrifugation step, both proteins were predominantly found in plasma, in line to what had previously been reported for other F8-based fusion proteins, which were not trapped by leukocytes [(Doll *et al.*, 2013, Hemmerle *et al.*, 2014), Figure 2A].

The F8-IL12p40 C175S fusion protein was then submitted to PNGase F treatment. A loss in apparent mass in SDS-PAGE analysis was observed [Figure 2B and Supplementary Figure 1] and mass spectrometric analysis confirmed the complete removal of glycostructures [Figure 2D]. Deglycoslyation of F8-IL12p40 C175S under native conditions did not alter protein homogeneity or thermal stability profiles [Figure 2C,E]. After removal of PNGase F, F8-IL12p40 C175S was radioiodinated and injected into F9 tumor-bearing mice. In this case, a preferential tumor uptake could be observed [Figure 2F], which however did not match the selectivity of the parental F8 diabody [Figure 1J].

Cloning, expression and characterization of F8-IL12p40 C175S mutants

In order to study whether the tumor targeting properties of F8-IL12p40 C175S could be improved by removal of glycosylation sites, nine Asn-to-Gln mutants were generated by site-directed mutagenesis. The resulting protein variants, which lacked either one, three or all four glycosylation sites, were cloned into the pcDNA 3.1 (+) vector and produced by transient gene expression [Figure 3]. Two of the mutants (termed 234Q and 1234Q), however, could not be expressed at acceptable yields and purity, thus preventing further analysis. The remaining seven mutants were purified to homogeneity and were shown to display a biochemical quality comparable to the one of the parental F8-IL12p40 C175S fusion protein, as assessed by SDS-PAGE analysis and size-exclusion chromatography.

Analysis of F8-IL12p40 C175S and its mutants by ESI/LC-MS and N-acetyl neuraminic acid quantification

An initial mass spectrometric analysis of F8-IL12p40 C175S mutants [Figure 4, Supplementary Table I] revealed the presence on N-linked glycans only on position N198 and N298. The triple mutant 134Q displayed a mass close to the theoretical molecular weight predicted from its amino acid composition, indicating that position N110 is not glycosylated. Additionally, the observed masses of mutants 3Q and 123Q as well as 4Q and 124Q were virtually identical (taking Asn-to-Gln mutations into account), which implies the absence of glycans at position N25. Upon partial deglycosylation, the observed masses of the deglycosylated 3Q and 4Q species were found to be near their theoretical molecular mass.

The mass differences observed in the mass spectra of the partially deglycosylated 3Q and 4Q mutants allowed us to elucidate putative N-glycan structures via a database search (details are given in the Material and Methods section of this manuscript) and rational considerations based on genomic knowledge of CHO cell-specific N-glycosylation. Specifically, mutant 3Q implied the presence of a bi-antennary complex N-glycan with two terminal sialic acids on position N298 while mutant 4Q suggested high-mannose type N-glycans on position N198 [Supplementary Figure 2]. The presence of terminal sialylation was further investigated by HPLC-based quantification of N-acteyl neuraminic acid (NeuNAc) [Supplementary Figure 3]. Indeed, this orthogonal analysis confirmed the existence of two terminal NeuNAc residues per F8-IL12p40 C175S monomers featuring N-linked glycans on position N298, providing further support for our glycostructure prediction.

Activity assessment and *in vivo* characterization of purified F8-IL12p40 mutants

The purified F8-IL12p40 C175S mutants revealed similar antigen binding capacity and IL12 inhibitory activity as the parental protein [Figure 5]. A quantitative biodistribution study in F9 tumor-bearing mice using radioiodinated preparations of the mutants, however, did not exhibit a recovery to tumor-homing activity [Figure 5]. Indeed, tissue distribution profiles were similar for the seven proteins and largely comparable to the one observed for the parental F8-IL12p40 C175S immunocytokine [Figure 1G].

Protein analysis by circular dichroism (CD) spectroscopy

Protein fold and thermal stability of the F8-IL12p40 C175S preparations tested *in vivo* were examined with circular dichroism (CD) spectroscopy. The obtained spectra [Figure 6] of glycosylation site-mutants were comparable to the parental and natively deglycosylated F8-IL12p40 C175S and show a characteristic topology for anti-parallel β sheet immunoglobulin-domains with global maxima below 205 nm and around 230-233 nm as well as a global minimum at 216-218 nm. The observed anti-parallel β sheet profile is in agreement with published crystal structures for human p40 in human IL12 (Yoon *et al.*, 2000) (72% sequence homology with mouse IL12p40) and other human antibodies in diabody format (Perisic *et al.*, 1994).

Close examination of the CD spectra show that protein variants mutated in position 3Q and 4Q show lower MRE values within this wavelength range. However, clear differences in the overall protein fold were difficult to assess by these initial wavelength scans.

By contrast, thermal denaturation curves [Figure 6] monitored at 217 nm revealed that the tested glycosylation-site mutants indeed deviated from F8-IL12p40 C175S. Not surprisingly, mutations on positions N25 and N110, found to be non-glycosylated in our MS analysis, had very little impact on thermal stability and exhibited similar melting temperatures as the parental protein. The mutant 3Q and 123Q displayed biphasic denaturation/unfolding curves whereby the first transition occurred already at around 40 to 45°C.

The denaturation curves of the triple mutants 124Q and 134Q and, to a lesser extent also of 4Q, strongly deviated from the parental protein indicating that these mutations impair F8-IL12p40 C175S stability or folding. By contrast, native deglycosylation with PNGase F did not reduce the melting temperature of F8-IL12p40 C175S [Figure 2E].

Europe PMC Funders Author Manuscripts

Discussion

In this article, the impact of glycosylation on the properties of the F8-IL12p40 fusion protein was systematically studied, by enzymatic deglycosylation and by one or more Asn-to-Gln substitutions within predicted N-glycosylation sequence motives. In total, we characterized the parental protein and 8 derivatives in terms of their biochemical properties and tumor targeting performance in quantitative biodistribution studies, using radioiodinated protein preparations.

A comparative evaluation of the parental protein, the deglycosylated analogue and seven site-specific mutants revealed comparable antigen-binding profiles (as assessed by BIAcore analysis). However, some of the mutants (i.e., those with Asn-to-Gln substitution at positions N198 and N298) displayed a substantially reduced thermal stability, while other mutants (e.g., single N25Q and N110Q substitutions) did not exhibit changes in denaturation profiles, as assessed by circular dichroism. The impact of glycosylation site mutations on thermal stability is difficult to predict *a priori* and needs to be experimentally measured.

Protein glycosylation may have both positive and negative influences on the development of antibody-based biotherapeutics. In some case, glycosylation may confer improved solubility and stability to therapeutic proteins, thus enhancing their functional properties. However, some glycoforms (e.g., high-mannose carbohydrates or complex N-glycans lacking sialic acid at terminal positions) may be preferentially captured by the asialoglycoprotein receptor or mannose receptors, with a negative impact on pharmacokinetic and tissue distribution properties (Venetz, et al., 2015). Additionally, some glycoproteins rely on N-linked glycans for correct folding and trafficking through the endoplasmic reticulum (Helenius and Aebi, 2001).

Enzymatic deglycosylation may represent an option for producing homogenous protein preparations, but its industrial application remains challenging, both in terms of PNGase F costs and of Good-Manufacture-Practice (GMP) compliance.

Unlike tumor antigen-specific antibodies in IgG format, which need N-linked glycosylation at N297 for efficient recruitment of NK cells and antibody-dependent cell cytotoxicity (Nimmerjahn and Ravetch, 2008), biotherapeutic agents incorporating antibody fragments as pharmacodelivery vehicles typically display acceptable functional performance in the absence of glycosylation (Bootz and Neri, 2016, Pasche and Neri, 2012). In the interest of protein homogeneity and predictable *in vivo* performance, the removal of ‘problematic’ N-glycan structures from glycoprotein payloads by mutation remains therefore attractive but needs to be investigated with respect to protein stability and function.

The work presented in this article suggests that a combination of biochemical analysis, Asn mutation studies and quantitative biodistribution experiments may guide researchers for the development of armed antibodies, capable of preferential localization at the site of disease. As most targets for ligand-based pharmacodelivery are located on the abluminal aspect of blood vessels, a prolonged circulatory residence time and a preferential extravasation at the site of disease [e.g., in tumor blood vessels or in inflamed tissue; (Bootz and Neri, 2016,

Hess *et al.*, 2014, Jain, 1990)] represent important contributors to biopharmaceutical performance.

Materials and methods

Cell lines

CHO-S cells (Invitrogen) were cultivated in PowerCHO medium (Lonza) supplemented with 8 mM Ultraglutamine, HT supplement (GIBCO) and antibiotic-antimycotic solution (GIBCO) at 37°C. For protein production, CHO cells were cultured at 31°C in a 1:1 mixture of PowerCHO medium and ProCHO medium (Lonza) both supplemented as described above. For IL12p40 activity assessment, splenocytes, freshly harvested from C57BL/6 mice were cultured in RPMI 1640 medium (GIBCO) supplemented with 10% foetal bovine serum (FBS) at 37°C, 5% CO_2, 95% humidity.

Animals

For animal experiments, female OHB 129Sv mice were obtained from Charles River. The experiments described in this article were performed under the project license “Tumor targeting” (Bew. Nr. 27/2015), issued to Dario Neri by the local cantonal authority (Veterinäramt des Kantons Zürich).

Protein production and characterization

The genes coding for the F8-IL12p40 mutants were generated using site directed mutagenesis of the gene encoding the parental protein, which was recently published (Bootz, et al., 2015). The final sequences [Supplementary Figure 4A,B] were digested by NheI (NEB) and NotI (NEB) and ligated into doubly digested pcDNA3.1 vector (Invitrogen). The corresponding fusion proteins were expressed using polyethylenimine-mediated transient gene expression in CHO-S cells. Cell culture supernatants were harvested six days after cell transfection and proteins were purified by Protein A affinity chromatography (Sino Biological), exploiting binding of the VH domain of F8 to Protein A, as previously described (Sasso *et al.*, 1991). Subsequently, product quality was assessed by SDS-PAGE, size-exclusion chromatography using a Superdex 200 column (10/300GL, GE Healthcare, Little Chalfont, UK) and by surface plasmon resonance analysis (BIAcore) on an EDA-coated CM5 sensor chip (GE Healthcare).

Deglycosylation of F8-IL12p40 C175S, 3Q and 4Q

Deglycosylation of F8-IL12p40 C175S, 3Q and 4Q (0.4 mg/mL protein) was performed under non-denaturing conditions using Peptide-N-Glycanase F (PNGaseF, NEB, 250 U per μg protein, incubation at 37 °C for 8-10 h).

For MS analysis, the reaction was performed in PBS using glycerol free PNGase F. After deglycosylation, the proteins were found to be partially deglycosylated, which allowed for simultaneous analysis of deglycosylated and native protein species within the same MS spectrum.

Complete protein deglycosylation for *in vivo* targeting assessment was achieved using PNGase stored in glycerol and the corresponding Glycobuffer (NEB). To remove PNGase F and glycerol afterwards, the deglycosylated immunocytokine was purified using protein A coupled sepharose, eluted with triethylamine and dialyzed to PBS.

Protein analysis by LC-MS

Native and deglycosylated protein samples were diluted in PBS to a concentration of 0.1 mg/mL and analyzed with an Acquity UPLC H class system equipped with a Acquity BEH300 C4 column (2.1 x 50 mm, 1.7µm particle size) sequentially coupled to a Waters Xevo G2-XS QTOF ESI mass analyzer. The applied LC-method was designed to remove salts from the samples without further separation of the protein constituents. Briefly, 10 µL samples were injected and chromatographically desalted by isocratic elution using a mobile phase consisting 95% solvent A (0.1% formic acid in water) and 5% solvent B (0.1% formic acid in acetonitrile) at a constant flow rate of 0.4 mL/min. After 1.5 min, the salt-free sample was eluted by stepwise gradient elution to 95% solvent B within 4.5 min (10% change solvent B every 30s then back to 95% solvent A within 30s) and subjected to ESI mass analysis. Three wash cycles (linear change to 95% solvent B within 2.25min and back to 95% A) were implemented to remove residual protein from the column between sample runs.

The resulting spectra were deconvoluted using the software MassLynx v4.1. The mass difference between native and deglycosylated protein species was used to predict possible glycan structures with the help of a database search of the 'Consortium of Functional genomics' database integrated in the used Glycoworkbench v2.0 software (Ceroni *et al.*, 2008). Notably, 19.0 Da was added to the observed mass differences in order to account for the addition of one H_20 molecule (as a consequence of the PNGase F reaction) and protonation, which typically occurs during the ionization of salt-free glycoprotein samples. Putative glycan structure were thereafter selected based on available genomic information of CHO K1-specific N-linked glycosylation (Xu *et al.*, 2011). The presence of terminally sialylated N-glycans was confirmed by HPLC quantification of neuraminic acids as described below.

N-acteyl neuraminic acid (NeuNAc) quantification

Terminal sialic acids were released by mild hydrolysis in 0.5 M $NaHSO_4$ (Sigma Aldrich) during 40 min at 80°C. Hydrolysed sialic acids were then derivatized with an excess of o-phenylenediamine (OPD, Sigma Aldrich) in the same buffer for 2 h at 80°C to enable subsequent fluorescence detection. A standard series of N-acetyl-neuraminic acid (Sigma Aldrich) was simultaneous processed for calibration. RP-HPLC separation of sialic acid-OPD derivatives was performed with a Hitachi Lachrom D-7000 HPLC-system equipped with an Xterra® 5 µm, 4.6 x150 mm C18 column (Waters) and a L-7480 fluorescence detector. Isocratic elution with a mobile phase of 7% solvent A (0.15% 1-butylamine, 0.5% phosphoric acid and 1% tetrahydrofurane in water) and 93% solvent B (50% solvent A and 50% acetonitrile) at a flow rate of 1 mL/min was used to chromatographically isolate OPD-labelled NeuNAc as previously described (Anumula, 1995). Fluorescence detection at Ex/Em 280/425 nm then allowed the quantification of terminal NeuNAc in the tested F8-

IL12p40 C175S mutant samples. Protein concentrations used for NeuNAc-to-F8-IL12p40 C175S monomer normalization were measured using a NanoDrop 2000c system.

Activity assessment of proteins

Spleens obtained from healthy female C57BL/6 mice were harvested, homogenized in 3mL medium and isolated using a cell strainer (40 mm; BD Falcon, Becton, Dickinson and Company). After a centrifugation step at 250 g ($g = 9.8\ m\ s^{-2}$) for 5 min, medium was removed and cells were resuspended in 3 mL red blood cell lysis buffer (Sigma Aldrich) After incubation for 10 min at room temperature, lysis was stopped by adding 10 mL of medium followed by a second isolation step through a cell strainer. The resulting flow-through containing the isolated splenocytes was centrifuged for 5 min at 250 g and the supernatant was removed. Subsequently, splenocytes were resuspended in medium to achieve a final concentration of $5 \cdot 10^6$ cells per mL. Afterwards, $5 \cdot 10^5$ cells were seeded into wells of a 96-well plate and covered with 100 µL medium containing 5 ng/mL recombinant murine IL12 (PeproTech EC Ltd., London, UK). Different concentrations of F8-IL12p40 (ranging from 0.3 mg/mL to $3 \cdot 10^8$ mg/mL) were added to each well except for the negative control wells. Cells were incubated at 37°C, 5% CO2, 95% humidity. After 48 h, cell supernatants were harvested and analyzed for Interferon-γ (IFNγ) expression by sandwich enzyme-linked immunosorbent assay, using a rat-anti-mouse IFN γ (Clone R4-6A2, eBioscience) for capture and a polyclonal biotinylated rabbit-anti-mouse IFN γ (PeproTech) for detection.

Whole blood incubation assay

Blood from healthy, twelve weeks old C57/BL6 was collected in syringes containing 50 µL ACD-anticoagulant (Sigma-Aldrich) and transferred to EDTA tubes (BD Microtainer) in fractions of 200 µL. Either 39.3 nM or 393 nM of radiolabeled F8-IL12p40 C175S or radiolabeled F8 diabody were added. Blood samples were incubated for 1 h at 37 °C and then centrifuged for 5 min at 2000 g. 90 µL of the supernatant and 100 µL of the cell pellet were transferred to radiation counting tubes and measured for radioactivity using a Packard Cobra γ counter.

Radioiodination of proteins and quantitative biodistribution studies

150 µg of protein (0.375 mg/mL) were radiolabeled with 200 µCi of sodium iodide-125 (Perkin Elmer) using the iodogen method. Pre-coated iodination tubes (Pierce) were equilibrated with 1 mL of PBS. Subsequently, 100 µL of PBS and the respective volume of NaI-125 were added directly to the bottom of the tube, mixed and incubated for 5 min,while slightly swirling the tube every 30 s. The solution containing the activated iodine was transferred to a tube containing 150 µg of protein, followed by incubation for 5 min. The solution was loaded onto a BSA blocked PD-10 column (GE Healthcare. The labelled protein was eluted with 3 mL PBS and collected in fractions of 0.5 mL.

For quantitative biodistribution studies, F9 tumor-bearing mice were injected (*i.v.*) with 10 µg radiolabeled protein preparation. 24 h after injection, organs were harvested, weighed and radioactivity was measured using the Packard Cobra γ counter.

Protein analysis by circular dichroic (CD) spectroscopy

All protein samples analyzed by CD were dialyzed for at least 16 h at 4°C to 10 mM NaCl, 10 mM Na_2HPO_4 at pH 7.5. The samples were then diluted to 0.180 mg/mL with dialysis buffer, which was used for background correction of the respective CD measurements. The samples were transferred to a 2 mm quartz glass cuvette and inserted in the AVIV CD spectrophotometer (Model 430) before initial wavelength scans in the range of 260 nm to 195 nm were performed. Thermal denaturation was monitored at 217 nm because at this wavelength, the largest change in MRE was observed when comparing samples at 25°C and 95°C (data not shown). Protein denaturation was achieved by heating the samples in 1°C / min steps with 30 s averaging time. After background correction to eliminate buffer effects, the data was processed as described in (Greenfield, 2006).

Supplementary Material

Refer to Web version on PubMed Central for supplementary material.

Acknowledgments

The authors would like to thank Sabine Studer for the introduction to the CD spectrometer and Dr. Chia-wei Lin for useful discussion regarding the glycan structure predictions.

Funding

This work was supported by ETH Zürich, Swiss National Science Foundation, KTI MedTech Project and by an ERC Advanced Grant (ZAUBERKUGEL).

References

Alewine C, Hassan R, Pastan I. Advances in anticancer immunotoxin therapy. The oncologist. 2015; 20:176–185. First published on, DOI: 10.1634/theoncologist.2014-0358 [PubMed: 25561510]

Anumula KR. Rapid quantitative determination of sialic acids in glycoproteins by high-performance liquid chromatography with a sensitive fluorescence detection. Analytical biochemistry. 1995; 230:24–30. First published on, DOI: 10.1006/abio.1995.1432 [PubMed: 8585625]

Becker JC, Pancook JD, Gillies SD, Mendelsohn J, Reisfeld RA. Eradication of human hepatic and pulmonary melanoma metastases in SCID mice by antibody-interleukin 2 fusion proteins. Proc Natl Acad Sci U S A. 1996; 93:2702–2707. First published on, [PubMed: 8610104]

Bootz F, Neri D. Immunocytokines: a novel class of products for the treatment of chronic inflammation and autoimmune conditions. Drug discovery today. 2016; 21:180–189. First published on, DOI: 10.1016/j.drudis.2015.10.012 [PubMed: 26526566]

Bootz F, Schmid AS, Neri D. Alternatively Spliced EDA Domain of Fibronectin Is a Target for Pharmacodelivery Applications in Inflammatory Bowel Disease. Inflammatory bowel diseases. 2015; First published on 2015/05/23, doi: 10.1097/MIB.0000000000000440

Bosslet K, Straub R, Blumrich M, Czech J, Gerken M, Sperker B, Kroemer HK, Gesson JP, Koch M, Monneret C. Elucidation of the mechanism enabling tumor selective prodrug monotherapy. Cancer Res. 1998; 58:1195–1201. First published on, [PubMed: 9515805]

Casi G, Neri D. Noninternalizing targeted cytotoxics for cancer therapy. Molecular pharmaceutics. 2015; 12:1880–1884. First published on, DOI: 10.1021/mp500798y [PubMed: 25738312]

Ceroni A, Maass K, Geyer H, Geyer R, Dell A, Haslam SM. GlycoWorkbench: a tool for the computer-assisted annotation of mass spectra of glycans. J Proteome Res. 2008; 7:1650–1659. First published on, DOI: 10.1021/pr7008252 [PubMed: 18311910]

Chari RV, Miller ML, Widdison WC. Antibody-drug conjugates: an emerging concept in cancer therapy. Angewandte Chemie. 2014; 53:3796–3827. First published on, DOI: 10.1002/anie.201307628 [PubMed: 24677743]

Constantinou A, Epenetos AA, Hreczuk-Hirst D, Jain S, Deonarain MP. Modulation of antibody pharmacokinetics by chemical polysialylation. Bioconjugate chemistry. 2008; 19:643–650. First published on, DOI: 10.1021/bc700319r [PubMed: 18307285]

Constantinou A, Epenetos AA, Hreczuk-Hirst D, Jain S, Wright M, Chester KA, Deonarain MP. Site-specific polysialylation of an antitumor single-chain Fv fragment. Bioconjugate chemistry. 2009; 20:924–931. First published on, DOI: 10.1021/bc8005122 [PubMed: 19402707]

Doll F, Schwager K, Hemmerle T, Neri D. Murine analogues of etanercept and of F8-IL10 inhibit the progression of collagen-induced arthritis in the mouse. Arthritis research & therapy. 2013; 15:R138. First published on 2013/12/03, doi: 10.1186/ar4319 [PubMed: 24289726]

Gillessen S, Carvajal D, Ling P, Podlaski FJ, Stremlo DL, Familletti PC, Gubler U, Presky DH, Stern AS, Gately MK. Mouse interleukin-12 (IL-12) p40 homodimer: a potent IL-12 antagonist. Eur J Immunol. 1995; 25:200–206. First published on 1995/01/01, DOI: 10.1002/eji.1830250133 [PubMed: 7843232]

Greenfield NJ. Using circular dichroism spectra to estimate protein secondary structure. Nat Protoc. 2006; 1:2876–2890. First published on, DOI: 10.1038/nprot.2006.202 [PubMed: 17406547]

Gregoriadis G, Jain S, Papaioannou I, Laing P. Improving the therapeutic efficacy of peptides and proteins: a role for polysialic acids. Int J Pharm. 2005; 300:125–130. First published on, DOI: 10.1016/j.ijpharm.2005.06.007 [PubMed: 16046256]

Halin C, Gafner V, Villani ME, Borsi L, Berndt A, Kosmehl H, Zardi L, Neri D. Synergistic therapeutic effects of a tumor targeting antibody fragment, fused to interleukin 12 and to tumor necrosis factor alpha. Cancer Res. 2003; 63:3202–3210. First published on 2003/06/18. [PubMed: 12810649]

Helenius A, Aebi M. Intracellular functions of N-linked glycans. Science. 2001; 291:2364–2369. First published on, [PubMed: 11269317]

Hemmerle T, Doll F, Neri D. Antibody-based delivery of IL4 to the neovasculature cures mice with arthritis. Proc Natl Acad Sci U S A. 2014; 111:12008–12012. First published on 2014/08/06, DOI: 10.1073/pnas.1402783111 [PubMed: 25092334]

Hemmerle T, Neri D. The antibody-based targeted delivery of interleukin-4 and 12 to the tumor neovasculature eradicates tumors in three mouse models of cancer. International journal of cancer Journal international du cancer. 2014; 134:467–477. First published on 2013/07/03, DOI: 10.1002/ijc.28359 [PubMed: 23818211]

Hemmerle T, Wulhfard S, Neri D. A critical evaluation of the tumor-targeting properties of bispecific antibodies based on quantitative biodistribution data. Protein engineering, design & selection : PEDS. 2012; First published on 2012/09/14, doi: 10.1093/protein/gzs061

Hess C, Venetz D, Neri D. Emerging classes of armed antibody therapeutics against cancer. Medchemcomm. 2014; 5:408–431. First published on, DOI: 10.1039/C3md00360d

Jain RK. Vascular and interstitial barriers to delivery of therapeutic agents in tumors. Cancer Metastasis Rev. 1990; 9:253–266. First published on, [PubMed: 2292138]

Kim DJ, Kim KS, Song MY, Seo SH, Kim SJ, Yang BG, Jang MH, Sung YC. Delivery of IL-12p40 ameliorates DSS-induced colitis by suppressing IL-17A expression and inflammation in the intestinal mucosa. Clinical immunology. 2012; 144:190–199. First published on 2012/07/28, DOI: 10.1016/j.clim.2012.06.009 [PubMed: 22836084]

Kontermann RE. Antibody-cytokine fusion proteins. Arch Biochem Biophys. 2012; 526:194–205. First published on, DOI: 10.1016/j.abb.2012.03.001 [PubMed: 22445675]

Krall N, Scheuermann J, Neri D. Small targeted cytotoxics: current state and promises from DNA-encoded chemical libraries. Angewandte Chemie. 2013; 52:1384–1402. First published on, DOI: 10.1002/anie.201204631 [PubMed: 23296451]

Lee SJ, Evers S, Roeder D, Parlow AF, Risteli J, Risteli L, Lee YC, Feizi T, Langen H, Nussenzweig MC. Mannose receptor-mediated regulation of serum glycoprotein homeostasis. Science. 2002; 295:1898–1901. First published on, DOI: 10.1126/science.1069540 [PubMed: 11884756]

Melkko S, Halin C, Borsi L, Zardi L, Neri D. An antibody-calmodulin fusion protein reveals a functional dependence between macromolecular isoelectric point and tumor targeting performance. Int J Radiat Oncol Biol Phys. 2002; 54:1485–1490. First published on 2002/12/03. [PubMed: 12459375]

Morell AG, Gregoriadis G, Scheinberg IH, Hickman J, Ashwell G. The role of sialic acid in determining the survival of glycoproteins in the circulation. J Biol Chem. 1971; 246:1461–1467. First published on. [PubMed: 5545089]

Muller N, Derouazi M, Van Tilborgh F, Wulhfard S, Hacker DL, Jordan M, Wurm FM. Scalable transient gene expression in Chinese hamster ovary cells in instrumented and non-instrumented cultivation systems. Biotechnology letters. 2007; 29:703–711. First published on 2007/02/21, DOI: 10.1007/s10529-006-9298-x [PubMed: 17310326]

Niesner U, Halin C, Lozzi L, Gunthert M, Neri P, Wunderli-Allenspach H, Zardi L, Neri D. Quantitation of the tumor-targeting properties of antibody fragments conjugated to cell-permeating HIV-1 TAT peptides. Bioconjugate chemistry. 2002; 13:729–736. First published on 2002/07/18. [PubMed: 12121127]

Nimmerjahn F, Ravetch JV. Anti-inflammatory actions of intravenous immunoglobulin. Annu Rev Immunol. 2008; 26:513–533. First published on, DOI: 10.1146/annurev.immunol.26.021607.090232 [PubMed: 18370923]

Pasche N, Neri D. Immunocytokines: a novel class of potent armed antibodies. Drug discovery today. 2012; 17:583–590. First published on 2012/02/01, DOI: 10.1016/j.drudis.2012.01.007 [PubMed: 22289353]

Perisic O, Webb PA, Holliger P, Winter G, Williams RL. Crystal structure of a diabody, a bivalent antibody fragment. Structure. 1994; 2:1217–1226. First published on. [PubMed: 7704531]

Poh S, Chelvam V, Low PS. Comparison of nanoparticle penetration into solid tumors and sites of inflammation: studies using targeted and nontargeted liposomes. Nanomedicine-Uk. 2015; 10:1439–1449. First published on, DOI: 10.2217/Nnm.14.237

Rybak JN, Roesli C, Kaspar M, Villa A, Neri D. The extra-domain A of fibronectin is a vascular marker of solid tumors and metastases. Cancer Res. 2007; 67:10948–10957. First published on 2007/11/17, DOI: 10.1158/0008-5472.CAN-07-1436 [PubMed: 18006840]

Sasso EH, Silverman GJ, Mannik M. Human IgA and IgG F(ab')2 that bind to staphylococcal protein A belong to the VHIII subgroup. Journal of immunology. 1991; 147:1877–1883. First published on 1991/09/15.

Schliemann C, Neri D. Antibody-based targeting of the tumor vasculature. Biochimica et biophysica acta. 2007; 1776:175–192. First published on 2007/10/09, DOI: 10.1016/j.bbcan.2007.08.002 [PubMed: 17920773]

Schwager K, Kaspar M, Bootz F, Marcolongo R, Paresce E, Neri D, Trachsel E. Preclinical characterization of DEKAVIL (F8-IL10), a novel clinical-stage immunocytokine which inhibits the progression of collagen-induced arthritis. Arthritis research & therapy. 2009; 11:R142. First published on 2009/09/29, doi: 10.1186/ar2814 [PubMed: 19781067]

Scott AM, Wolchok JD, Old LJ. Antibody therapy of cancer. Nat Rev Cancer. 2012; 12:278–287. First published on, DOI: 10.1038/nrc3236 [PubMed: 22437872]

Sievers EL, Senter PD. Antibody-drug conjugates in cancer therapy. Annu Rev Med. 2013; 64:15–29. First published on, DOI: 10.1146/annurev-med-050311-201823 [PubMed: 23043493]

Sinclair AM, Elliott S. Glycoengineering: the effect of glycosylation on the properties of therapeutic proteins. J Pharm Sci. 2005; 94:1626–1635. First published on, DOI: 10.1002/jps.20319 [PubMed: 15959882]

Sondel PM, Gillies SD. Current and Potential Uses of Immunocytokines as Cancer Immunotherapy. Antibodies (Basel). 2012; 1:149–171. First published on, DOI: 10.3390/antib1020149 [PubMed: 24634778]

Steiner M, Neri D. Antibody-Radionuclide Conjugates for Cancer Therapy: Historical Considerations and New Trends. Clinical Cancer Research. 2011; 17:6406–6416. First published on, DOI: 10.1158/1078-0432.Ccr-11-0483 [PubMed: 22003068]

van der Veldt AA, Hendrikse NH, Smit EF, Mooijer MP, Rijnders AY, Gerritsen WR, van der Hoeven JJ, Windhorst AD, Lammertsma AA, Lubberink M. Biodistribution and radiation dosimetry of

11C-labelled docetaxel in cancer patients. European journal of nuclear medicine and molecular imaging. 2010; 37:1950–1958. First published on, DOI: 10.1007/s00259-010-1489-y [PubMed: 20508935]

Venetz D, Hess C, Lin CW, Aebi M, Neri D. Glycosylation profiles determine extravasation and disease-targeting properties of armed antibodies. Proc Natl Acad Sci U S A. 2015; 112:2000–2005. First published on 2015/02/04. DOI: 10.1073/pnas.1416694112 [PubMed: 25646460]

Villa A, Trachsel E, Kaspar M, Schliemann C, Sommavilla R, Rybak JN, Rosli C, Borsi L, Neri D. A high-affinity human monoclonal antibody specific to the alternatively spliced EDA domain of fibronectin efficiently targets tumor neovasculature in vivo. International journal of cancer Journal international du cancer. 2008; 122:2405–2413. First published on 2008/02/14. DOI: 10.1002/ijc.23408 [PubMed: 18271006]

Xu X, Nagarajan H, Lewis NE, Pan S, Cai Z, Liu X, Chen W, Xie M, Wang W, Hammond S, et al. The genomic sequence of the Chinese hamster ovary (CHO)-K1 cell line. Nature biotechnology. 2011; 29:735–741. First published on, DOI: 10.1038/nbt.1932

Yoon C, Johnston SC, Tang J, Stahl M, Tobin JF, Somers WS. Charged residues dominate a unique interlocking topography in the heterodimeric cytokine interleukin-12. EMBO J. 2000; 19:3530–3541. First published on, DOI: 10.1093/emboj/19.14.3530 [PubMed: 10899108]

Europe PMC Funders Author Manuscripts

Europe PMC Funders Author Manuscripts

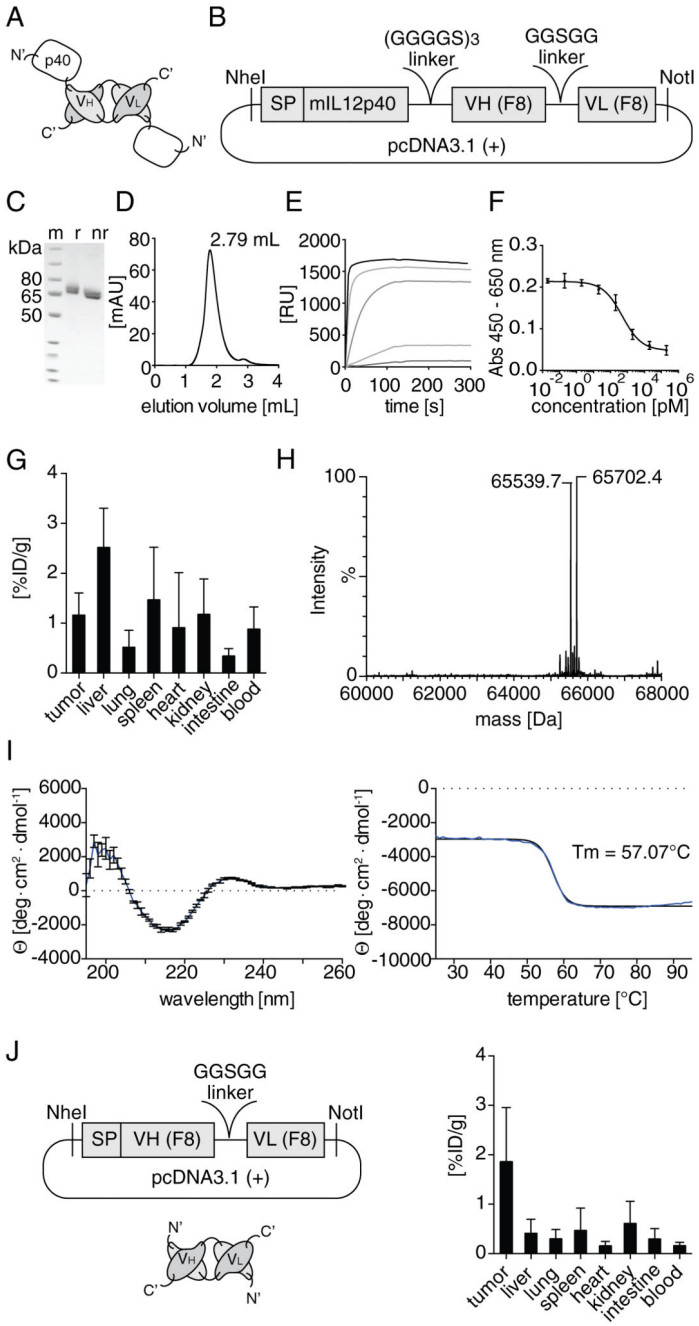

Figure 1.

A, Schematic representation of the domain structure of F8-IL12p40 C175S. **B**, Overview of the essential elements of the plasmid for the mammalian expression F8-IL12p40 C175S. The purified protein was characterized by: **C**, SDS-PAGE analysis (m: marker; r: reducing conditions; nr: non-reducing conditions); **D**, Size exclusion chromatography; **E**, Surface plasmon resonance analysis on a BIAcore CM5 chip coated with the antigen (EDA). **F**, Plot of F8-IL12p40 C175S activity assessment, based on the inhibition of IL12-induced IFNγ secretion of splenocytes. **G**, Quantitative biodistribution analysis of F8-IL12p40 C175S in

F9 teratocarcinoma bearing mice, 24 h after injection of 10 μg radioiodinated protein preparation. Radioactivity content of each organ is shown in percent injected dose per gram [%ID/g]. **H**, Mass spectrometric analysis (ESI/LC-MS). **I**, Wavelength scan and thermal denaturation curve assessed by CD spectroscopy. **J,** Schematic representation of the F8 diabody, corresponding expression vector and quantitative biodistribution profile.

Europe PMC Funders Author Manuscripts

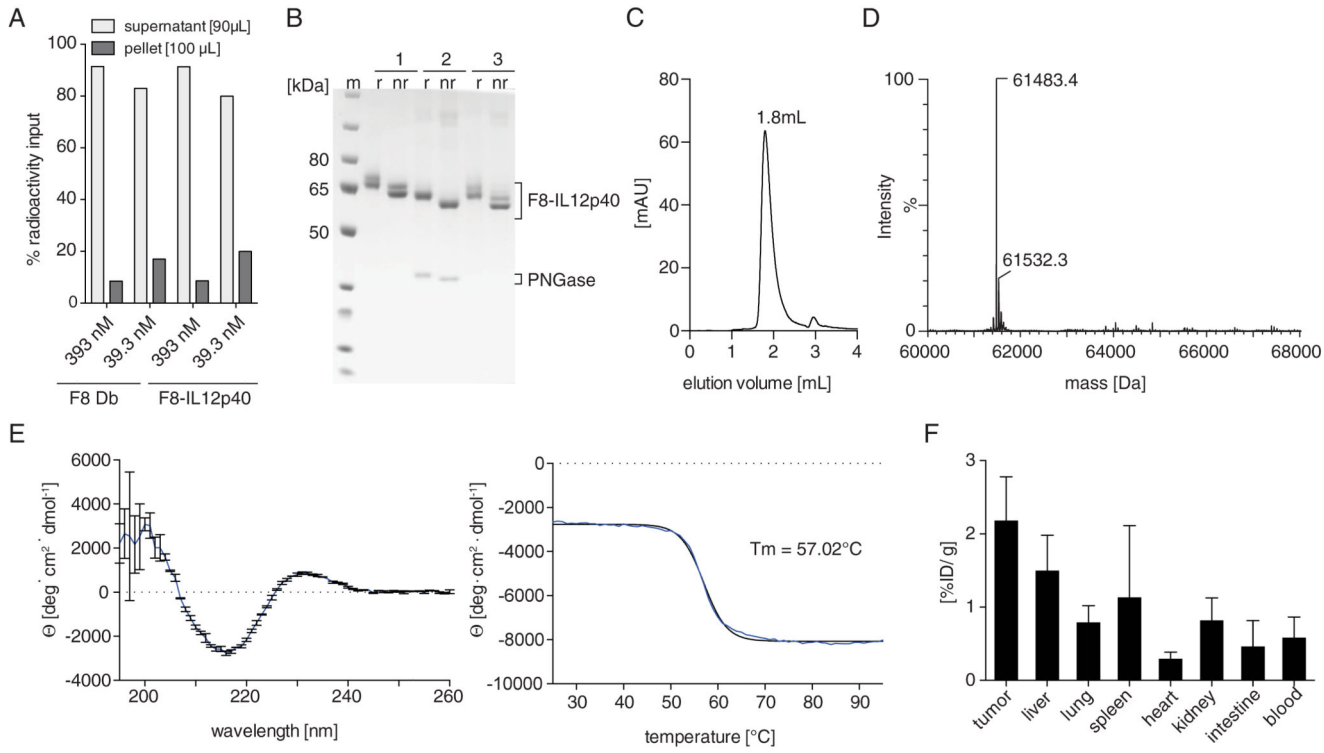

Figure 2.

A, Comparative blood incubation assay of radiolabeled preparations of F8-IL12p40 C175S and F8 diabody. Equimolar concentrations of the proteins were incubated in murine blood for 1 hour at 37°C. After centrifugation, radioactivity content of supernatant and pellet was measured. **B**, SDS-PAGE analysis of purified F8-IL12p40 C175S before (1) and after (2) deglycosylation using PNGase F. The deglycosylated product was purified over protein A (3) to separate it from the PNGase F enzyme (m: marker; r: reducing conditions; nr: non-reducing conditions). **C**, Size exclusion chromatogram. **D**, Mass spectrometric analysis (ESI/LC-MS). **E**, Wavelength scan and thermal denaturation curve assessed by CD spectroscopy. **F**, Quantitative biodistribution analysis F8-IL12p40 C175S in F9 teratocarcinoma bearing mice, 24 h after injection of 10 µg radioiodinated protein preparation. Radioactivity content of each organ is shown as percent injected dose per gram [%ID/g].

Europe PMC Funders Author Manuscripts

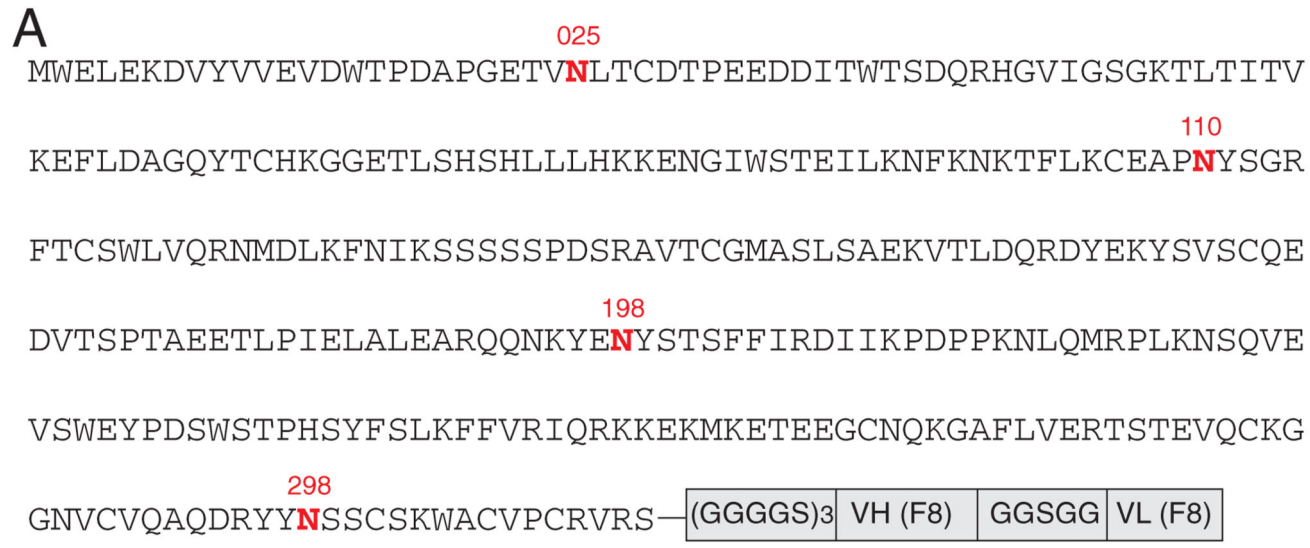

B

i)

mutant name	mutation
1Q	N025Q
2Q	N110Q
3Q	N198Q
4Q	N298Q

ii)

mutant name	mutations
123Q	N025Q, N110Q, N198Q
124Q	N025Q, N110Q, N298Q
134Q	N025Q, N198Q, N298Q
234Q	N110Q, N198Q, N298Q
1234Q	N025Q, N110Q, N198Q, N198Q

Figure 3.

A, Schematic representation of F8-IL12p40 C175S and its four glycosylation sites. **B**, Description of generated mutants lacking i) one or ii) more glycosylation sites.

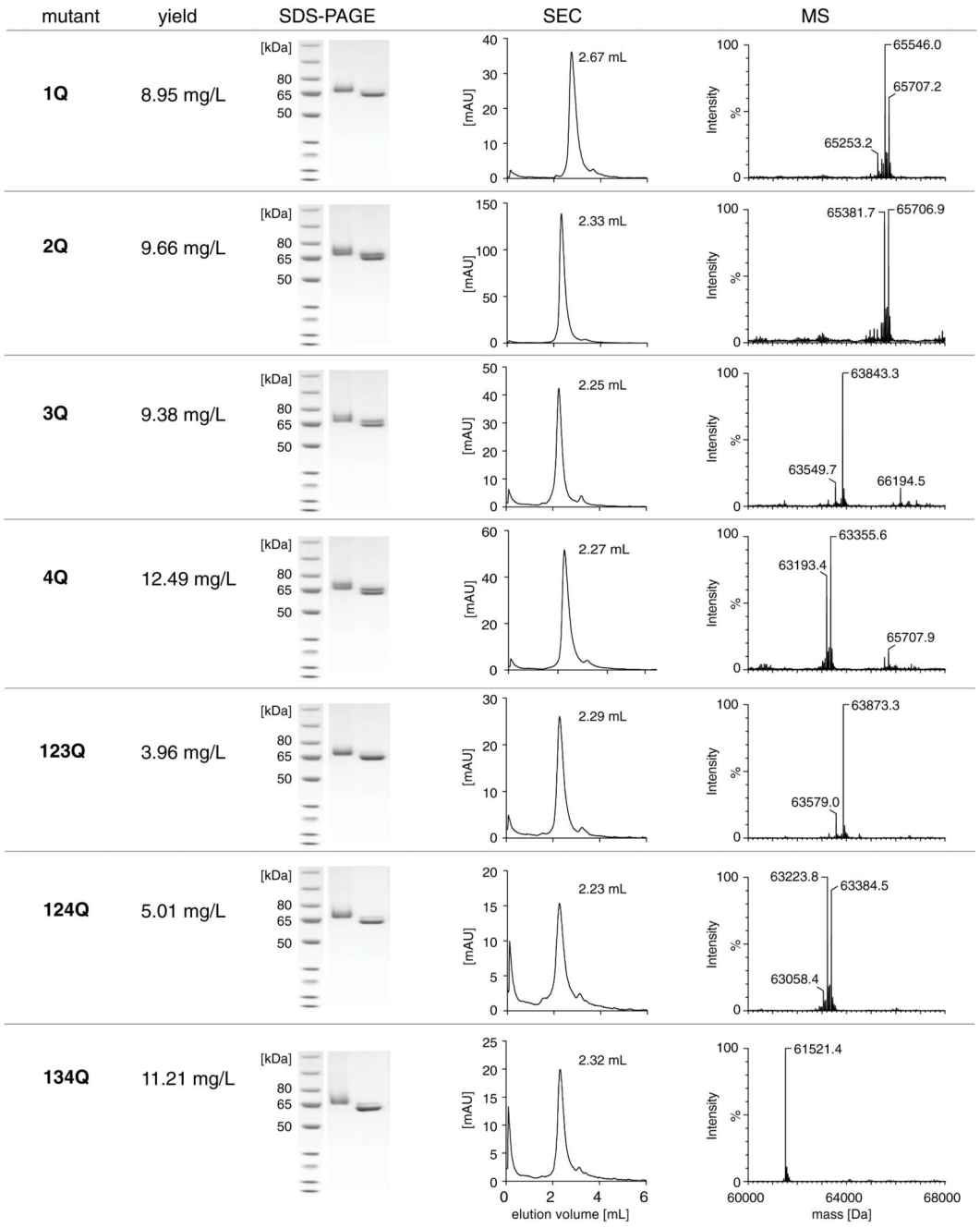

Figure 4.

Characterization of purified F8-IL12p40 C175S mutants in terms of production yield, SDS-PAGE analysis, size-exclusion chromatograms and mass spectrometric analysis (ESI/LC-MS).

Europe PMC Funders Author Manuscripts

Europe PMC Funders Author Manuscripts

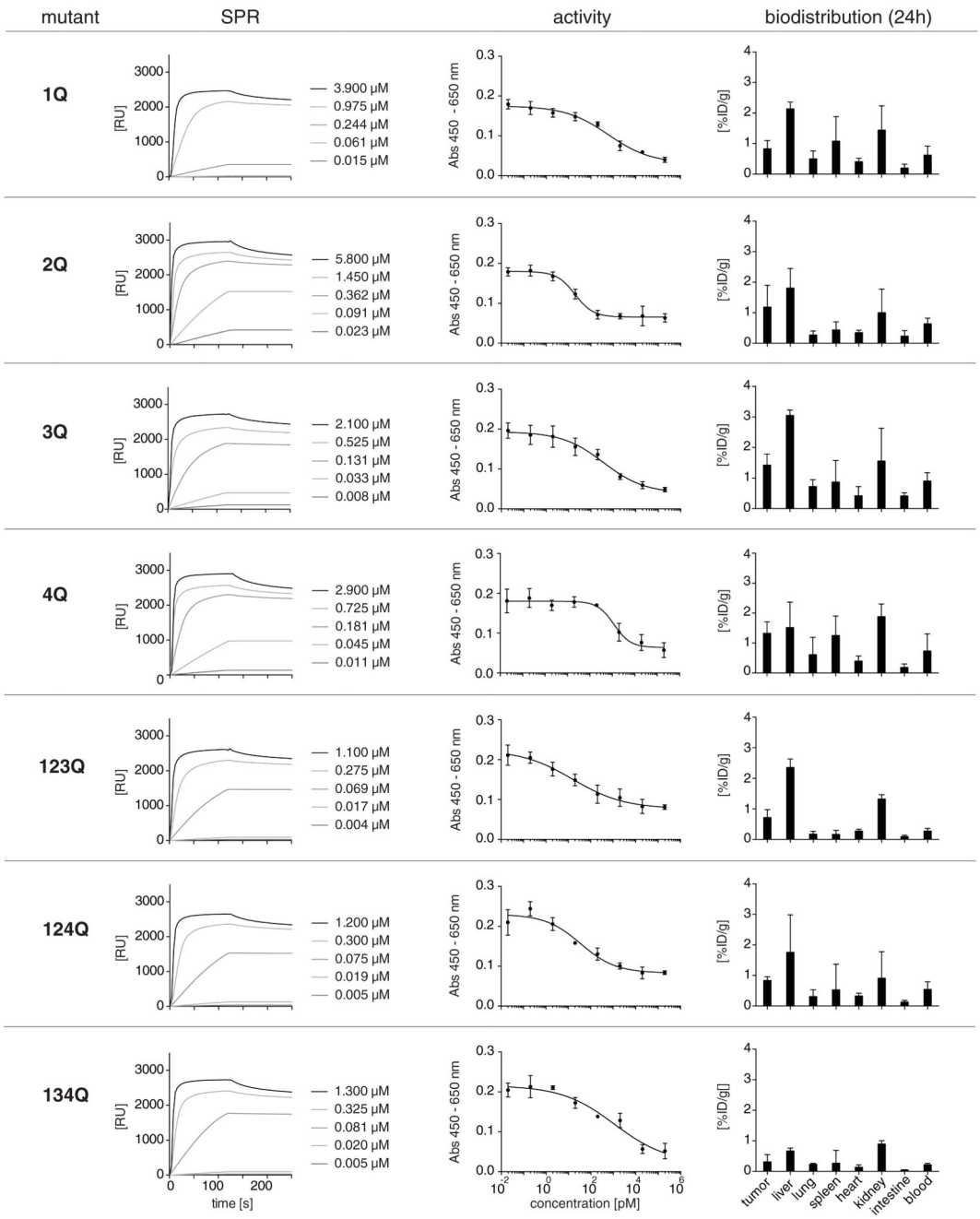

Figure 5.

Characterization of purified F8-IL12p40 C175S mutants in terms of surface plasmon resonance analysis, inhibition of IL12 activity and quantitative biodistribution profiles.

Europe PMC Funders Author Manuscripts

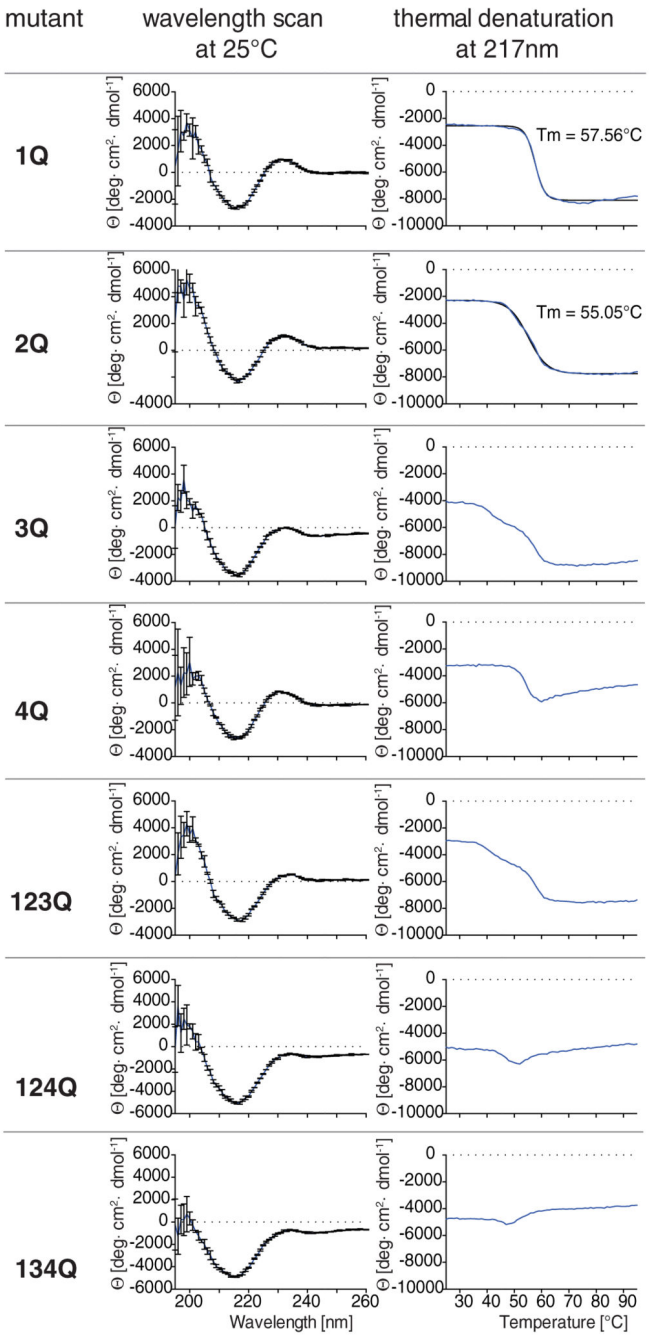

Figure 6.

Circular dichroism (CD) spectroscopy of F8-IL12p40 C175S mutants, showing wavelength scans at 25°C, as well as thermal denaturation profiles, monitored at 217 nm.